The simulation of ultrasonic imaging in the case of the objects with a complex geometry

R. Raišutis, L. Mažeika

Prof. K. Baršauskas Ultrasound Institute

Kaunas University of Technology

1.Introduction

The main objective of the ultrasonic non-destructive testing (NDT) applications is to detect dangerous defects in the various constructions. The parameters and geometry of defects is very important information determining lifetime of constructions or components. In conventional ultrasonic NDT methods, based on the measurement of the amplitude and delay time of reflected signal are used. Such an approach enables evaluate size and position of defects only approximately. Most accurate is time – of the flight - diffraction (TOFD) technique, which allows measuring depth of defects. Additional application of the SAFT or tomographic algorithms enables to increase accuracy even more [1,2,3]. Nevertheless, practical applications of these methods usually are complicated due to a lack of a sufficiently accurate information about ultrasound propagation conditions, such as the propagation velocity, angle, wave fronts and etc. Additional problem arises due to the fact that basic algorithms of these techniques are developed for the direct reflections only [1,2,3]. On the other hand, due to the object geometry or limited access very widely the signals reflected from the bottom or mode conversion signals are used. The successful application of all these signals in tomographic processing may increase the accuracy essentially. The development of such algorithms using only experimental data is very complicated because it is impossible to determine sensitivity of the technique to the uncertainty of the input parameters. This problem can be solved developing special method and software that enables to simulate NDT data acquisition process, taking into account material parameters, transducer characteristics, diffraction and refraction phenomena.

Such models are used in other institutions like CEA (France), BAM (German) and others. Usually they are based on complicated numerical approach, which requires essential computer resources [4,5,6].

The objectives of this work was to develop relatively fast NDT simulation model, which enables to take into account not only direct reflection from defects, but specular reflection from object boundaries also. This task may be divided in some parts:

- selection of corresponding diffraction model;
- development of the specular reflection evaluation method;
- development of the NDT simulation algorithm;
- development image analysis method taking into accounts the specular reflections and the object geometry.

2.The object under investigation

There are a lot of test objects in industry and it is impossible to develop such an universal model. Our investigation was limited to the case of the planar homogenous object (Fig.1), which can correspond, for example, to testing of welded plates.
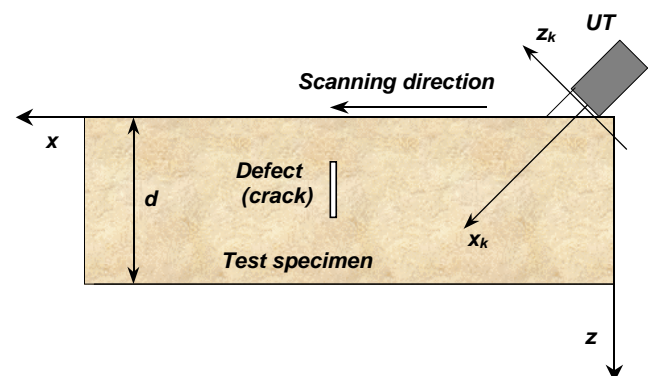

Fig.1. **The object under investigation. *UT* is the ultrasonic transducer; *d* is the thickness of the specimen; x_k, z_k is the coordinate system with respect to the transducer; *x, z* is the absolute coordinate system**

As defects we assumed the cracks with different orientation with respect to the surface of the object. According to the NDT procedure, test of such a plate is performed scanning the transducer and measuring reflected signal at each position. The measured data usually are presented in the form of B-scan. So the simulation procedure must perform all the separations on the virtual simulated object. The parameters of the model must be ultrasound velocity, thickness of the object, transducer diameter, pulse response and refraction angle, scanning distance and step.

3.The model for simulation of the ultrasonic NDT

The complete modelling of the described above ultrasonic NDT procedure can be performed in the following steps:
1. Modeling of the excitation signal;
2. Ultrasonic transducer field simulation;
3. Modeling of the test object with defects;
4. Calculation of the possible reflections, taking into account object boundaries.

The excitation signal was simulated as radio pulse with the asymmetric Gaussian envelope. The number of periods of the signal can be selected thus simulating transducers with different damping.

The next step is to simulate a diffracted ultrasonic field taking into account transducer characteristics and material properties. For simulation of ultrasonic fields several methods can be used:

- Methods based on direct application of Huyghens' principle.
- Methods, based on finite elements and finite differences;
- Methods, based on application of the angular spectrum.

The first group of methods calculates the ultrasonic field using the Huyghens' principle. The Rayleigh's equation expresses the velocity potential at a field point as the sum of contributions from elementary Huyghens' sources, each radiating a hemispherical wave into a medium. The direct application of this approach requires a big amount of integration procedures and from this point of wiew application of it for calculation of the pulse response is complicated. Nevertheless, there are many modification of this approach developed for the case of disk shape transducer [7,8,9,10]. Of course, it is complicated to apply this method for calculation of reflected signals.

The second group of methods is based on numerical approach used very widely for calculation of vibrations of mechanical constructions. The basis of these methods is the division of the physical domain into sub-domains, or elements, within which exact or approximate solutions can be obtained. Later using integration procedure the propagation of ultrasonic wave can be simulated. The advantage of numerical methods is that they are flexible with respect to the geometry of the object. It is possible to simulate not only propagation of the wave in homogeneous medium, but to observe the transformation of the waves on the boundaries and defects also. The main problem is that the number of elements and consequently the number of equations which is necessary to solve depends on the wavelength. The shorter wave length, the smaller elements must be. So in the case of higher frequencies the duration of calculations increases essentially and requires big computing resources [11,12].

The third group of ultrasonic field simulation techniques is based on application of the angular spectrum or Fourier decomposition method. With this method a monochromatic pressure distribution over a plane surface is decomposed into an equivalent two-dimensional spectrum of plane waves. The propagation of this wave field to another parallel plane is modelled by multiplying each spectral component by the appropriate phase factor [13]. But this method requires big computational resources also.

From the short analysis follows that simplest methods, used for the ultrasonic field simulation are based on direct application of Huyghens' principle, but it is necessary to extend them to calculation of the reflected signals. The approach described in [14,15,16,17] was selected as the basis for simulation of ultrasonic field.

In the next chapter the model for the calculation of the reflections will be presented, the problems, associated with realisation of the model will be analysed and the proposals for the solution of the problems will be made.

3.1. The approach for evaluation of a reflected signal

The three basic cases can be separated in the reflected signal (Fig.2): the direct reflection from the defect (transducer - defect - transducer), the specular reflection (transducer - bottom - defect - bottom - transducer) and mixed reflection (transducer-bottom-defect-transducer).
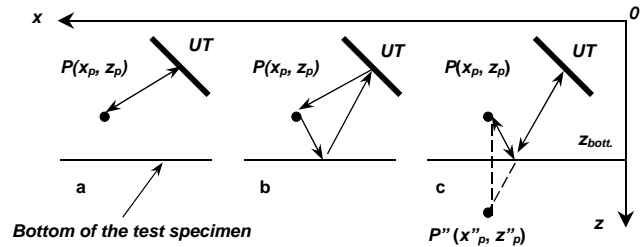

Fig.2.   **Calculation steps of the reflections. a, b, c is the direct, mixed and specular reflections from the real point reflector $P(x_p, z_p)$; $P''(x''_p, z''_p)$ is the virtual position of reflector; $z_{bott.}$ is the bottom surface of the specimen; UT is the ultrasonic transducer.**

These three cases were selected because they are most typical in practical ultrasonic NDT. The searching for direct reflection is used during tests of various objects. The signal reflected from the bottom is widely exploited in the weld testing. The mixed reflection case enables to simulate signal from the corners of the object and vertical cracks.

The direct reflection can be calculated as the convolution of the transmitted signal and pulse response of the transducer the given for reflector position:

$$S_1(t, x_p, z_p) = (u(t) \otimes h(t, x_p, z_p)) \otimes h(t, x_p, z_p), (1)$$

where $\otimes$ denotes convolution operation, $u(t)$ is the excitation signal, $h(t, x_p, z_p)$ is the spatial pulse response for the point reflector $P(x_p, z_p)$. The double convolution with the pulse response is used to calculate signal in a pulse echo mode.

The specular reflection is calculated in a similar way, only instead of a real position of the reflector the virtual mirror image of it is used:

$$S_3(t, x_p, z_p) = (u(t) \otimes h(t, x''_p, z''_p)) \otimes h(t, x''_p, z''_p), (2)$$

where $h(t, x''_p, z''_p)$ is the spatial pulse response for the virtual position of the point reflector $P''(t, x''_p, z''_p)$. The coordinates of the virtual position of the point reflector is calculated according to

$$x''_p = x_p,$$
$$z''_p = (z_{bott.} - z_p) + z_{bott.}$$ (3)

The beam path in the case of a mixed reflection has a part, corresponding both to direct and mirror reflections. So it can be calculated as

$$S_2(t, x_p, z_p) = (u(t) \otimes h(t, x''_p, z''_p)) \otimes h(t, x_p, z_p). (4)$$

The resultant received signal from the reflector $P(x_p, z_p)$. is calculated as superposition of all three reflections [18,19,20]:

$$S_P(t, x_p, z_p) = \sum_{n=1}^{3} S_n(t, x_p, z_p). (5)$$

The each defect can be presented as a group of point reflectors. In such a case a complete reflected signal can be calculated as a sum of signals reflected from all point reflectors:

$$S_\Sigma(t) = \sum_{k=1}^{N_p} S_{p_k} = \sum_{k=1}^{N_p} \sum_{n=1}^{3} S_n(t, x_p, z_p), \qquad (6)$$

where N_p is number of point reflectors.

So the NDT process simulation algorithm can be expressed as presented in Fig.3. The input parameters include information about test object and defects geometry, transducer orientation and ultrasound velocity.

Most important part of this algorithm is the convolution procedure, because it essentially influences the efficiency of the method in a sense of computing resources.
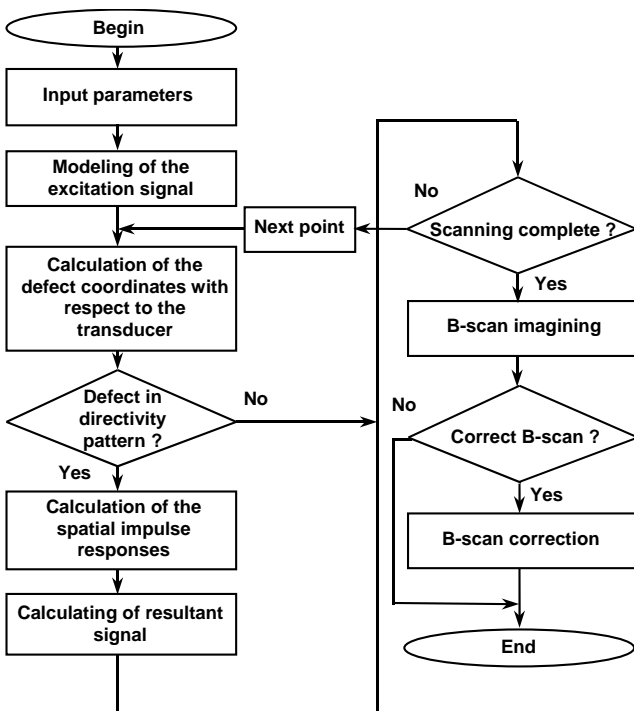

Fig. 3. Algorithm of the developed model.

Usually the convolution is performed using the Fourier transformation, because this method is faster then convolution in the time domain. For use of such an approach signals has to be sampled with the constant step Δt, which has to be small enough in order to get a sufficient accuracy in a far field of the transducer. This leads to the increase of number of discrete points used in convolution and, as consequence, increases a calculation time.

The modified method [15,16,17] used in our case allows calculate the pulse response of the transducer with a varying step in the time domain and in such a way enables to increase accuracy in the far field zone. The direct application of functions, sampled with a varying step in the Fourier transformation is impossible, but there is another advantage of selected method: the accuracy does not depend very much on the number of points. Because of that, it can be selected relatively small, in our case about

100. In the case of a pulse technique the excitation signal is short and can be sampled using a few hundreds points too. In such a case the convolution can be performed relatively fast in the time domain. Such an approach enabled to increase calculation speed essentially. The other steps of the algorithm are simple, that is, acquisition of calculated signals on the hard disk of the personal computer and presentation in the form of B-scan image.

4. The verification of the developed NDT simulation algorithm

The verification of the model was performed in a few steps. In the first step the reflections from the most typical crack like reflectors with different orientation were analyzed. In second step the comparison of the simulation results with the experimental data was performed.

4.1. Analysis of most typical reflectors.

The three types of reflectors were selected for analysis: the vertical crack in the middle of the object (Fig.4 a), the crack perpendicular to the ultrasonic beam (Fig.4 b) and the crack near the bottom of the object (Fig.4c).
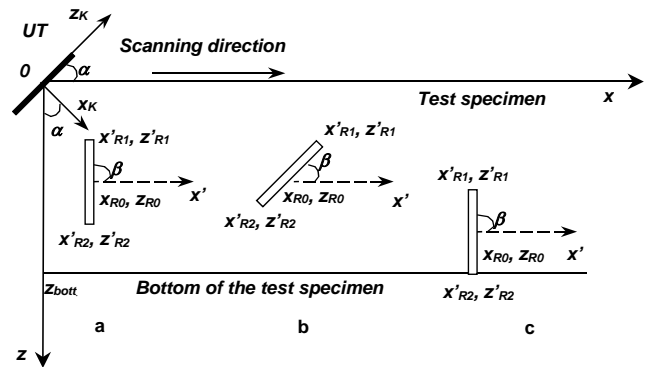

Fig. 4. **Reflectors selected for the verification of the model. a-vertical crack; b-crack perpendicular to the ultrasonic beam ; c-vertical crack at the bottom; *UT* is the ultrasonic transducer; x'_{R1}, z'_{R1} and x'_{R2}, z'_{R2} is the coordinates of the crack edges; x_{R0}, z_{R0} is the coordinates of the crack center; x_k, z_k is the coordinate system of the transducer; x, z is the absolute coordinate system; β is the crack orientation angle with x axis; α is the ultrasonic transducer orientation angle with respect x axis; $z_{bott.}$ is the coordinate of the bottom of test sample (equal to thickness of the specimen).**

The 45° transducer with a radius $R=2.5$ mm, and frequency $f=5$MHz was used for the simulations. The ultrasound velocity in the brass test specimen $c=5015$ m/s, thickness of the object $d=25$ mm. The contact technique was simulated. The scanning area over the object was 25 mm and step 0.1 mm. The simulated crack length was 4 mm. The sampling step of the signals was 0.01 µs. The simulation results are presented in Fig.5.

In the case of the vertical crack the strong signal as from the corner reflector can be seen (Fig.5 a,c signals 2). In the same images the small signals as diffracted wave from the edges of the crack can be separated (Fig.5 a,c signals 1). The diffracted waves can be recognised in the specular reflection too (Fig.5 a,c signals 3). In the case of
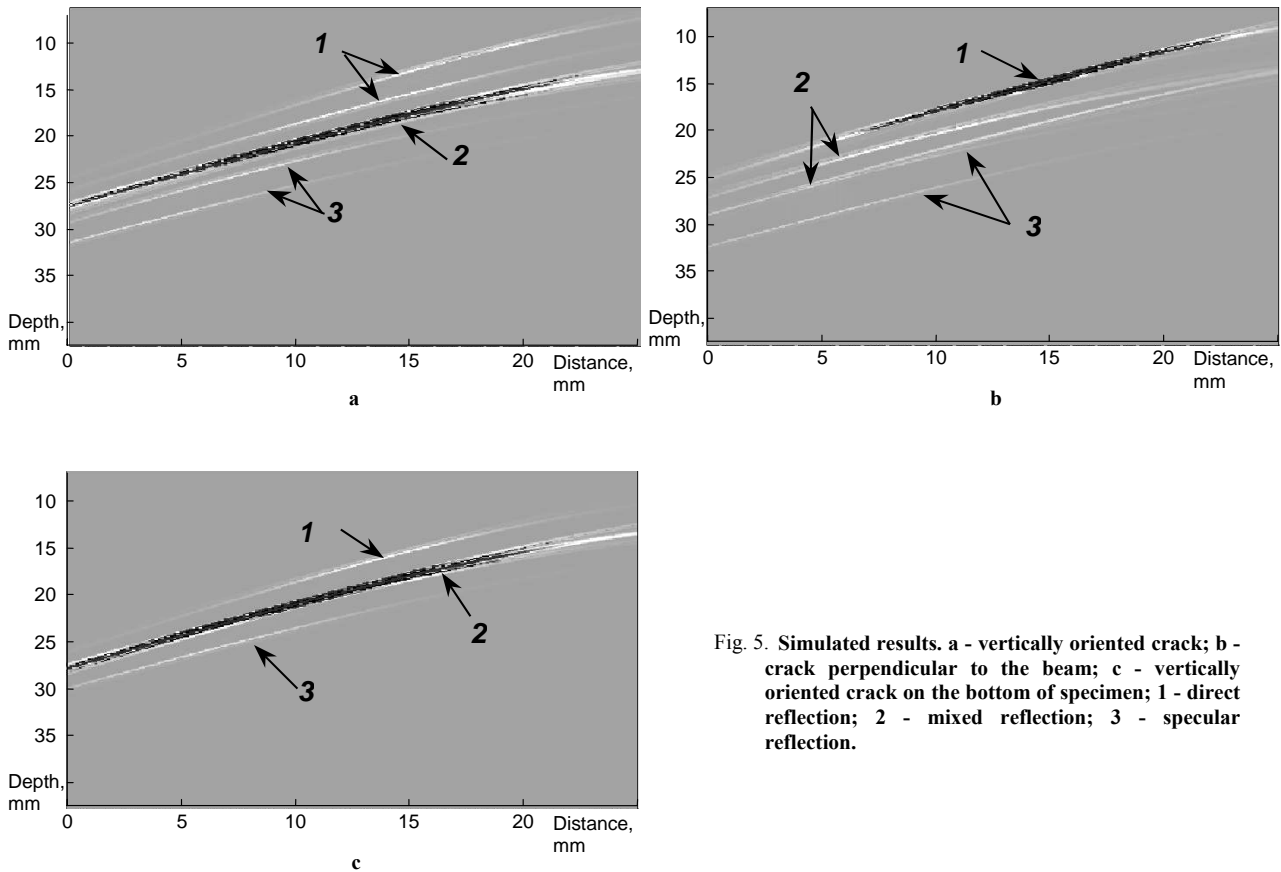
a

b

c

Fig. 5. **Simulated results. a - vertically oriented crack; b - crack perpendicular to the beam; c - vertically oriented crack on the bottom of specimen; 1 - direct reflection; 2 - mixed reflection; 3 - specular reflection.**

the crack, perpendicular to the ultrasonic beam the strong signal as from the plane reflector, can be seen (Fig.5 b signals 1). So, simulation results showed all characteristic signals observed in such cases.

4.2. Comparison with experimental data

The aluminum test sample with eight side-drilled holes was selected for experimental verification (Fig.6). The object length was 235 mm and the thickness d=95 mm. The testing was performed using contact technique with 48.5°, 2.5Mhz shear wave transducer. The piezoelement diameter was 15mm. The velocity of shear waves in the test specimen is c_t=3130 m/s. The test sample was scanned with step 0.235 mm. In such a way the measurements were performed in 1000 position. The experiments were taken using ultrasonic visualisation system "ULTRALAB-3" [21]. The sampling frequency of A/D converter was 40 MHz. The simulation and experimental results in the form of the B-scan images are presented in Fig.7. In general there is a good agreement between experimental and simulated data. For better comparison we calculated exact positions of detected reflectors and differences between experimental and simulated data. Such results are presented in Table 1. There σ_{an} is the absolute error of the transducers orientation angle, δ_{an} is the relative error of the transducer orientation angle, σ_{tn} is the absolute error of the reflection arriving time, δ_{tn} is the relative error of the arriving time of the reflected signal. The experimental results were taken as the reference value for evaluation of relative errors.
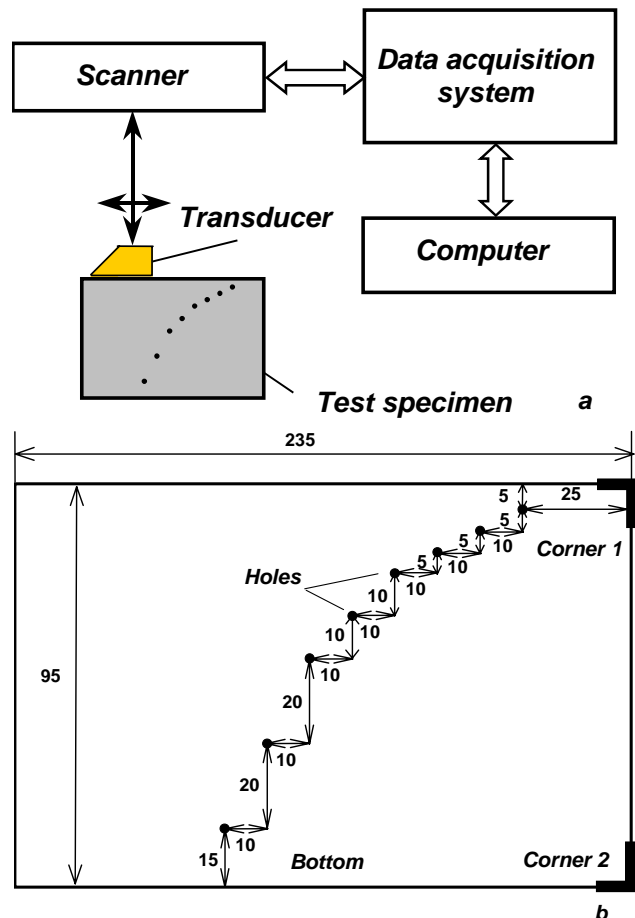

a

b

Fig. 6. **The experimental set-up (a) and aluminium test sample with side drilled holes (b)**

From Table 1 follows that there are errors between the transducer angle determined from experimental data and from the simulation data for holes.

Table 1. **Uncertainty values in simulation and experiment**

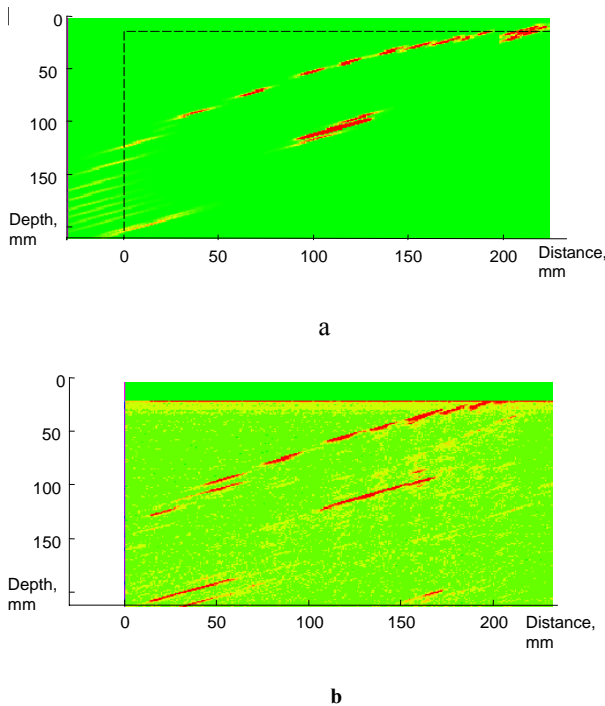| Hole No.	Simulation		Experiment		σ_{tn}, µs	δ_{tn}, %
	σ_{an}, °	δ_{an}, %	σ_{an}, °	δ_{an}, %		
1	-2,42	5,09	13,31	-28,86	0,734	4,519
2	0,64	-1,35	7,4	-16,01	-0,330	-1,594
3	0,58	-1,22	3,6	-7,81	-0,972	-3,865
4	0,44	-0,93	2,55	-5,53	-0,535	-1,771
5	-0,29	0,61	1,63	-3,53	0,548	1,404
6	0	0	0,68	-1,47	-0,447	-0,906
7	0,03	-0,06	0,24	-0,52	0,555	0,818
8	-0,03	0,06	-0,93	2,00	-0,042	-0,048

a

b

Fig.7. **B-scan images of the aluminium test sample (2D case): a – simulation, b – experiment;**
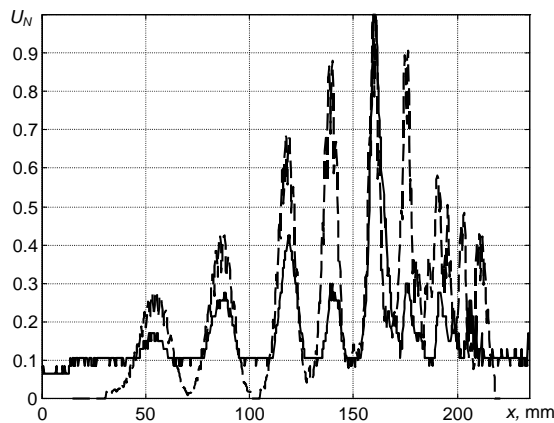

Fig. 8. **Echodynamical curves of the aluminium test sample (2D case): experimental data, -- simulated data;**

This can be explained as shear wave determination error. Additionally, there is a bigger error for the holes situated closer to the transducer.

For minimisation of these errors from experimental results, the modified value of ultrasound velocity was calculated 3062±24m/s. The new value of the recalculated transducer orientation angle is $\alpha = -47.14 \pm 0.33°$. Having those new values, a new simulation procedure was performed. The recalculated data are presented in the form of the echodynamic curve (Fig.8). The echodynamic curves is defined as maximum values in each A-scan. The Fig.8 shows that there is good correspondence in the position of reflections, but there is difference in the amplitude of the signals, especially in a near field zone. Partially it can be explained by the fact, that there 2D approach was used in the simulation and reflectors were point type. In the experiment side drill holes are closer to the liner a reflector, but not to the point type reflector.

5.2. The correction of the B-scan images

In a standard B-scan image the reflection does not correspond to a real reflector position. It is a question - how to obtain the real defect position from that image? The first step is to correct the B-scan image according to the transducer angle. This is performed shifting B-scan image in the shear - like mode (Fig.9). The shift distance N for each image point S_N is given by:

$$N = \frac{S_N \cdot \sin(\alpha)}{\Delta x};$$ (7)

where Δx is the transducer scanning step; α is the transducer angle

The areas having no information were filled with zeroes. The corrected in such a way B-scans of experimental and simulated data are presented in Fig.10 b, 10 e.

The second step is to correct positions of the specular reflections, exploiting position of the bottom of the test object. For that purpose, the image part, corresponding to the specular reflection, is overlapped on the part of the image corresponding to the direct reflection. The delay time from the virtual reflector at the bottom is found:

$$t_{bott.} = \frac{2 \cdot Z_{bott.}}{c \cdot \cos(\alpha)};$$ (8)

where Z_{bott} is the distance to the specimens bottom (mm), c is the ultrasound velocity (mm/µs).

The corrected positions t_n of the specular reflections in the time domain are recalculated:

$$t_n = 2 \cdot t_{bott.} - t_m;$$ (9)

where $t_{bott.}$ is the time of the flight from the bottom surface, t_m is the delay time of the specular reflections.

Using this expression we perform calculations in the zone $t_{min} \div 2 \cdot t_{bott.}$, if $t_{max} > 2 \cdot t_{bott.}$. In other case we perform calculations in the zone $t_{min} \div t_{max}$. These recalculated specular reflection positions are overlapped on the direct reflection positions. It results in cross-like images of direct and mirrors reflections which give more precise positions of the defects (Fig.10c, 10f). Simple multiplication of images data brings exact positions of the
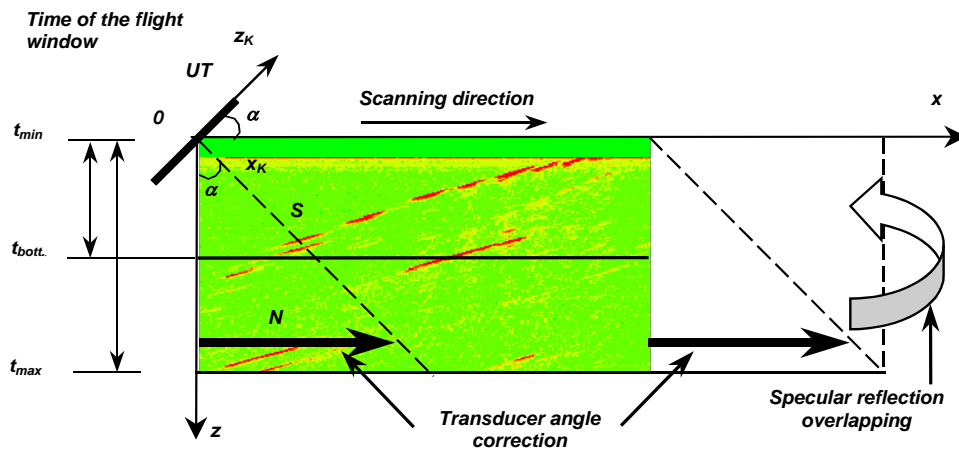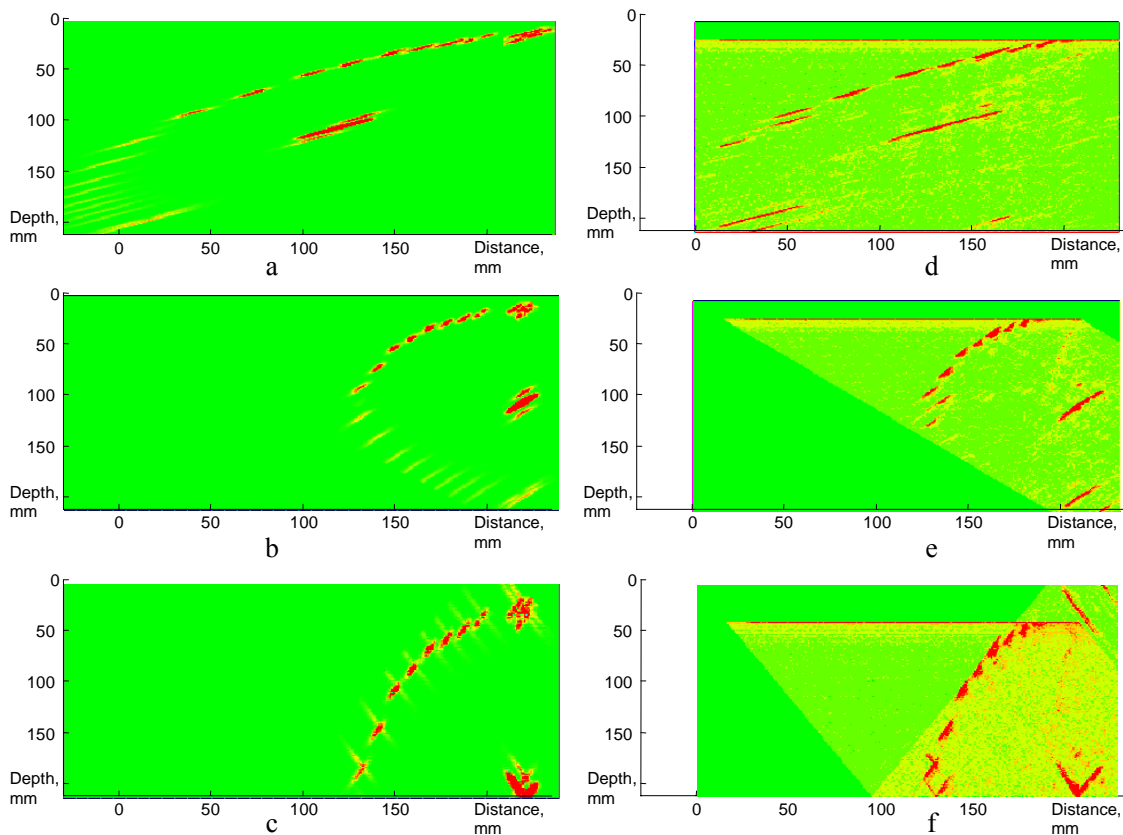
Fig. 9. **Correction of the B-scan images.**

Fig. 10. **Simulated (a-c) and experimental (d-f) B-scan images before and after corrections.**

reflector (Fig.11). Of course, for more precise analysis these data can be used in the SAFT and reflection tomography reconstruction techniques. The analysis of a mixed reflection is much more complicated and there are no good algorithms at the moment.

The demonstration of the simulation technique for weld inspection

For demonstration of the developed technique, the simulation of V-weld testing is presented (Fig.12). For the simulations the 45° angle transducer with the radius R=2.5 mm and the frequency f=2 MHz was used. The thickness

of the V-welded steel plate was d=20 mm. The ultrasound velocity in the test object was c_t=3,12 mm/μs. These data correspond to the steel N.302.

The scanning was performed over 75 mm distance with a step 0.1 mm. The two types of defects were simulated: lock of a fusion on the edge of the weld and on the bottom of the object a vertically oriented root crack. The simulated and corrected results are presented in Fig. 13.

The calculation, which has 750x3500 points, takes less then 10 minutes using PC with 366 MHz Pentium processor.
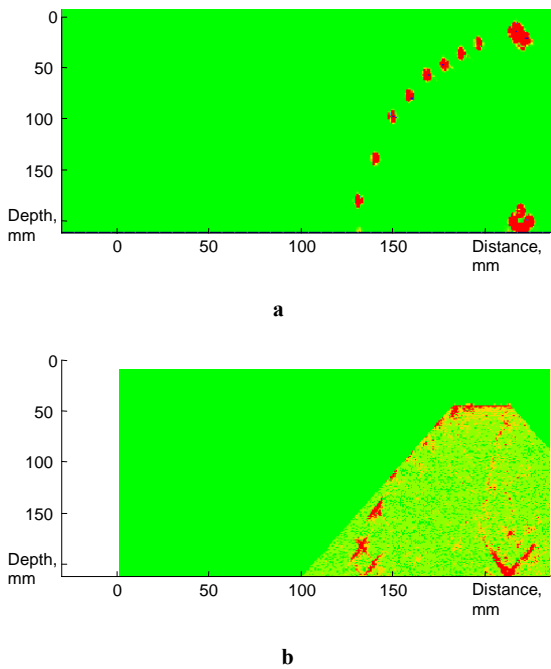
a

b

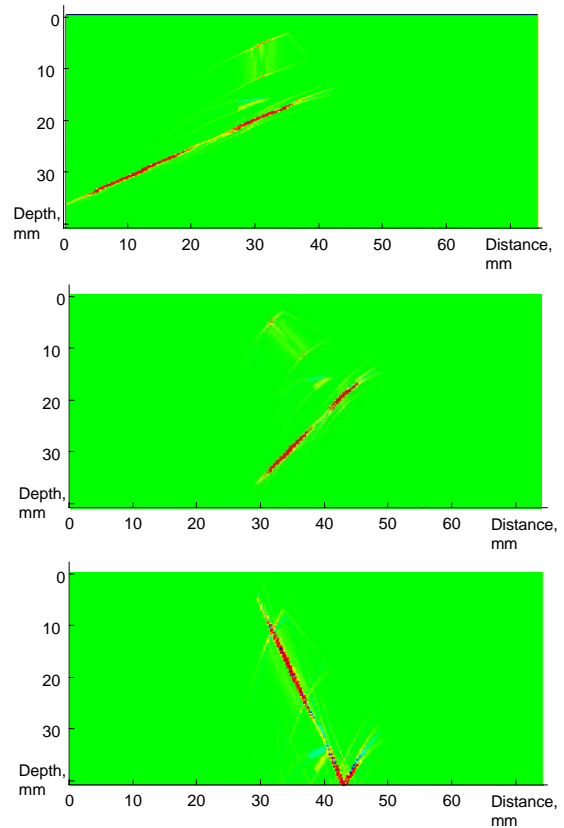Fig. 11. **Simulated (a) and experimental (b) B-scan images after corrections.**

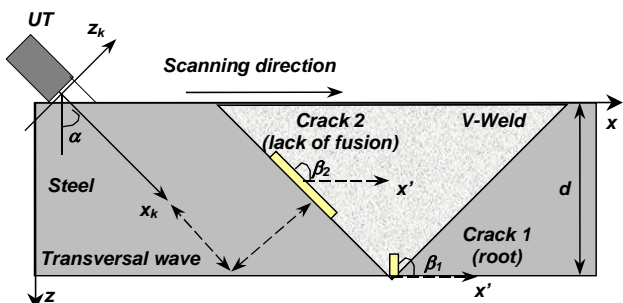Fig. 13. **B-scan images of V-weld simulation before and after corrections**

Fig. 12. **Simulation of the V-WELD testing:** *UT* **is the ultrasonic transducer,** *d* **is the thickness of the specimen,** *xk, zk* **is the coordinate system whith respect to the transducer,** *x,z* **is the absolute coordinate system,** *α* **is the ultrasonic transducer orientation angle with** *x* **axis,** *β* **is the crack orientation angle with respect to the** *x***-axis**

Conclusions

The ultrasonic NDT simulation method and fast algorithm have been developed. The developed technique enables to take into account direct, mixed, and specular reflections. The comparison of the simulated results with experimental, data has showed a good correspondence, especially in a far field zone. The B-scan image correction, taking into account specular reflections, have been developed.

The algorithms are relatively fast and enable simulate and analyse data by a conventional personal computer.

References

1. **Kino G.S.** Acoustic Imaging for non-destructive evaluation. Proc. of the IEEE 1979. Vol.67, No.4. P.510-525.

2. **Halmshaw R.** Non-destructive testing. London: Edward Arnold, 1991.

3. Non-destructive testing handbook, 2nd editon. Vol.7. Ultrasonic testing /Albert S. Virks, Robert E. Green, Paul McIntire. USA: American soc. for nondestructive testing. 1991. P.207-579.

4. **Wüstenberg H., Erhard A.** Approximative modeling for the practical application at ultrasonic inspection on page: the model. Report of BAM, April 1997.-VIII.4. www.ndt.net/article/wsho0597/ wuesten2/wuesten21.htm

5. **Calmon P., Lhemery A., Lecoeur-Taibi I.** Recent developments in ultrasonic NDT modelling in Civa. Roma 2000, 15th WCNDT, papers\idn639\idn639.htm, p.1-6.

6. **Scalia A., Sumbatyan M. A.** On efficient quantitative analysis in real-time ultrasonic detection of cracks. /Ultrasonics. 1999. Vol.37. P.239-245.

7. **Weight J. P.** Ultrasonic beam structures in fluid media. J. Acoust. Soc. Am. 1984. Vol.76, No. 4. P.1184-1191.

8. **Weight J. P.** A model for propagation of short pulses of ultrasound in a solid. J. Acoust. Soc. Am. 1987. Vol. 81, No. 4. P. 815-826.

9. **Weight J. P., Hayman A. J.** Observations of the propagation of very short ultrasonic pulses and their reflection by small targets. J. Acoust. Soc. Am. 1978. Vol. 63, No. 2. P. 396-404.

10. **Epasinghe K.** Simulation and visualization of ultrasound fields. University of Oslo., Department of informatics., 1 st August, 1997. P.1-134.

11. **Jensen F.B., Kuperman W.A., Porter M.B., Schmidt H.** Computational ocean acoustics. /AIP Press. 1993. P. 605.

12. **Shlager K. L., Schneider J.B.** A selective survey of the finite-difference time-domain literature. /IEEE antennas&propagation magazine. P.1-7.

13. **Schafer M.E., Lewin P.A.** Transducer characterization using the angular spectrum method. /J. Acoust. Soc. Am. 1989. Vol.85(5). P.2202-2214.

14. **Robinson D. E.** Near field transient radiation patterns for circular pistons. IEEE Trans. Acoust. Speech Sign. Proc. ASSP-22. 1974. P.395-405.

15. **Jasiūnienė E., Mažeika L**. The modified method for simulation of ultrasonic fields of disk shape transducer. /Ultragarsas. Kaunas: Technologija. 1999. No.3 (33). P.33-37.

16. **Kažys R., Mažeika L., Jasiūnienė E.** Application of ultrasonic reflection tomography for nondestructive evaluation of objects with a complex geometry. /J. Acoust. Soc. Am. 1999. Vol..105. No.2.(2). P.1360.

17. **Jasiūnienė E.** Ultragarsinės tomografijos taikymas defektų erdvinėms koordinatėms nustatyti. /Daktaro disertacija. Kaunas. 1999. P.37-43.

18. **Raillon R., Lecoeur-Taibi I.** Transient elastodynamic model for beam defect interaction: application to non-destructive testing. /Ultrasonics. 2000. Vol.38. P.527-530.

19. **Faur M., Morisseau P.** Ultrasonic data inversion for outer surface defects characterization.- 7th European conference on non-destructive testing Copenhagen, 26-29 May, 1998. P.2429-2431.

20. **Calmon P., Paradis L.** Ultrasonic NDT modeling of realistic configurations.- 7th European conference on non-destructive testing Copenhagen, 26-29 May, 1998. P.2993-3000.

21. **Kažys R., Mažeika L.,Voleišis A., Šliteris R., Kundrotas K., Augutis V.** Ultrasonic non-destructive testing system of journal bearings. /Ultragarsas. 1997. Nr. 1(27). P. 16-18.

R. Raišutis, L. Mažeika

Atspindžių nuo sudėtingos geometrijos objektų modeliavimas ir vizualizavimas

Reziume

Straipsnyje pateiktas neardančiųjų tyrimų modeliavimo algoritmas, įvertinantis objekto geometriją, ir jo matematinis aprašymas. Modelis įgalina gauti tiesioginius atspindžius nuo objekto dugno ir mišrius atspindžius nuo defekto. Modelis patikrintas skaičiuojant atspindžius nuo taškinio ir plokščiojo defekto, modeliavimo rezultatai patikrinti eksperimentiškai, atliktas jų lyginimas laike ir erdvėje. Pasiūlyta B tipo vaizdų koregavimo metodika.

Skaitmeniniu eksperimentu ištirtas dažnai praktinėje neardančiojoje kontrolėje pasitaikantis suvirinimo siūlės su dviem skirtingai orientuotais defektais atvejis.